ORIGINAL ARTICLE

Disturbed mitochondrial and peroxisomal dynamics due to loss of MFF causes Leigh-like encephalopathy, optic atrophy and peripheral neuropathy

Johannes Koch,[1] René G Feichtinger,[1] Peter Freisinger,[2] Mechthild Pies,[3] Falk Schrödl,[4] Arcangela Iuso,[5,6] Wolfgang Sperl,[1] Johannes A Mayr,[1] Holger Prokisch,[5,6] Tobias B Haack[5,6]

For numbered affiliations see end of article.

Correspondence to
Dr Johannes Koch, Department of Pediatrics, Paracelsus Medical University Salzburg, Muellner Hauptstr. 48, Salzburg 5020, Austria; j.koch@salk.at

Received 16 September 2015
Revised 25 November 2015
Accepted 12 December 2015
Published Online First 18 January 2016

ABSTRACT

Background Mitochondria are dynamic organelles which undergo continuous fission and fusion to maintain their diverse cellular functions. Components of the fission machinery are partly shared between mitochondria and peroxisomes, and inherited defects in two such components (dynamin-related protein (DRP1) and ganglioside-induced differentiation-associated protein 1 (GDAP1)) have been associated with human disease. Deficiency of a third component (mitochondrial fission factor, MFF) was recently reported in one index patient, rendering *MFF* another candidate disease gene within the expanding field of mitochondrial and peroxisomal dynamics. Here we investigated three new patients from two families with pathogenic mutations in *MFF*.

Methods The patients underwent clinical examination, brain MRI, and biochemical, cytological and molecular analyses, including exome sequencing.

Results The patients became symptomatic within the first year of life, exhibiting seizures, developmental delay and acquired microcephaly. Dysphagia, spasticity and optic and peripheral neuropathy developed subsequently. Brain MRI showed Leigh-like patterns with bilateral changes of the basal ganglia and subthalamic nucleus, suggestive of impaired mitochondrial energy metabolism. However, activities of mitochondrial respiratory chain complexes were found to be normal in skeletal muscle. Exome sequencing revealed three different biallelic loss-of-function variants in *MFF* in both index cases. Western blot studies of patient-derived fibroblasts indicated normal content of mitochondria and peroxisomes, whereas immunofluorescence staining revealed elongated mitochondria and peroxisomes. Furthermore, increased mitochondrial branching and an abnormal distribution of fission-mediating DRP1 were observed.

Conclusions Our findings establish MFF loss of function as a cause of disturbed mitochondrial and peroxisomal dynamics associated with early-onset Leigh-like basal ganglia disease. We suggest that, even if laboratory findings are not indicative of mitochondrial or peroxisomal dysfunction, the co-occurrence of optic and/or peripheral neuropathy with seizures warrants genetic testing for *MFF* mutations.

To cite: Koch J, Feichtinger RG, Freisinger P, *et al*. *J Med Genet* 2016;**53**:270–278.

INTRODUCTION

Mitochondria form a highly dynamic tubular network and undergo continuous fusion and fission to maintain their diverse cellular functions and organisation throughout the cell.[1–3] Whereas mitochondrial fusion promotes the exchange of organellar content, fission of mitochondria into small segments facilitates mitochondrial trafficking along the cytoskeleton. Mitochondrial trafficking is thought to be particularly important for the maintenance of cellular (energy) homeostasis in large, differentiated cell types such as neurons, and during cell division.[4] In addition, fission is essential for mitochondrial quality control, by separating out dysfunctional mitochondrial components targeted by the mitophagy machinery for subsequent degradation.[5] In peroxisomes, only fission has been demonstrated.[6] Mitochondria and peroxisomes exhibit a close functional relationship and share key components of their division machinery, including the dynamin-like GTPase dynamin-related protein 1 (DRP1) and its membrane adaptor proteins FIS1 (fission factor 1), MFF (mitochondrial fission factor) and GDAP1 (ganglioside-induced differentiation-associated protein 1).[2] DRP1 is recruited from the cytosol onto the outer membrane and mediates mitochondrial and peroxisomal fission through the formation of large multimeric spiral complexes that wrap around the tubule at the fission sites. Membrane fission is then realised by mechanochemical forces released upon guanosintriphosphat (GTP) hydrolysis.[7] Clinical features of the first patient with a defect in DRP1 and an early lethal course were reported by Waterham *et al* in 2007.[3] Mutations in *GDAP1* give rise to a Charcot–Marie Tooth disease (CMT) phenotype.[8] The outer membrane protein MFF is an essential component of the conserved membrane fission pathway of mitochondria and peroxisomes,[4 9] and presumably the major DRP1 receptor for organelle fission.[2] Knockdown of MFF results in mitochondrial elongation[9] and reduces the amount of DRP1 recruited to mitochondria.[10] Shamseldin *et al*[11] first identified a truncating mutation in *MFF* in a 4.5-year-old Saudi Arabian boy with delayed psychomotor development, spasticity, optic atrophy, and bilateral, increased signal intensities of the basal ganglia. His brother was mentioned as having similar psychomotor delay, without any further information given. Here we report detailed clinical, structural and functional data of three additional patients from two families with pathogenic *MFF* mutations.

METHODS

Human subjects

Patient 1 was recruited at a tertiary university children's hospital (Paracelsus Medical University, Salzburg) and patients 2 and 3 were recruited at Social Pediatric Center Frankfurt and a regional tertiary referral hospital (Klinikum Reutlingen), respectively. Both hospitals are specialised in mitochondrial diseases and are partners of the Bundesministerium für Bildung und Forschung (BMBF)-funded mitoNET research programme. All clinical data and samples were obtained with written informed consent of the patients' parents. The ethics committee of Technische Universität München approved the study.

Genetic studies

Exome sequencing was used to investigate the molecular basis of the mitochondrial disease presentation in patients 1 and 3. Genomic DNA was extracted from EDTA blood samples using standard protocols. Library preparation, bioinformatic analyses and prioritisation of candidate variants were performed as described previously.[12] Briefly, coding regions were enriched using a SureSelect Human All Exon 50 Mb V5 kit (Agilent) and the prepared libraries were sequenced on a HiSeq2500 platform (Illumina). Reads were aligned to genome assembly hg19 with Burrows–Wheeler Aligner (BWA, V.0.5.87.5) and genetic variation was detected using SAMtools (V.0.1.18), PINDEL (V.0.2.4t) and ExomeDepth (V.1.0.0). Of the target sequences, 98% were covered >20-fold.

Detected *MFF* variants were confirmed by Sanger sequencing. Genomic DNA was extracted from EDTA blood from all individuals but patient 2, from whom only a dry blood spot stored from newborn screening was available. Primer sequences and PCR conditions will be provided upon request.

Biochemical studies

Skeletal muscle tissues were homogenised in extraction buffer (20 mM Tris-HCl, pH 7.6, 250 mM sucrose, 40 mM KCl, 2 mM ethylene glycol tetraacetic acid) and centrifuged at 600 *g* to generate the postnuclear supernatant (600 *g* homogenate), which was used for measurement of mitochondrial respiratory chain (MRC) enzyme activities and western blot analysis. MRC enzyme activities were determined as published elsewhere.[13–15] Briefly, rotenone-sensitive complex I activity was measured spectrophotometrically as NADH/decylubiquinone oxidoreductase. The enzyme activities of citrate synthase, complex IV (ferrocytochrome c/oxygen oxidoreductase), and the oligomycin-sensitive ATPase activity of the F_1F_0 ATP synthase (complex V) were measured in buffer conditions described by Rustin *et al*.[16] Succinate dehydrogenase activity (complex II) was determined according to Rustin *et al* with slight modifications.[14] Buffer conditions and determination of complex III activity are described in ref 14. All spectrophotometric measurements were performed at 37°C. Long-range PCR of the mitochondrial DNA was performed with two independent sets of primers.[17]

Immunoblotting

For western blot analysis, a total of 10 µg protein of 600 *g* homogenate was separated on 10% acrylamide/bisacrylamide gels and transferred to nitrocellulose membranes using N-cyclohexyl-3-aminopropanesulfonic acid buffer. Washing and blocking procedures were performed as previously described.[14] The following primary antibody dilutions, incubation times and temperatures were used: monoclonal mouse anti-DRP1 (1:1000; 1 h, room temperature; Abcam, Cambridge, UK), monoclonal mouse antiporin (1:1000; 1 h, room temperature, MitoSciences) and polyclonal rabbit anticatalase (1:1000; 1 h, room temperature; Thermo Fisher Scientific). After washing, the membranes were incubated with secondary antibodies as follows: DRP1 and porin with labelled polymer-HRP (heat reactive protein)-antimouse (1:1000; 1 h, room temperature, EnVision kit, Dako) and catalase with labelled polymer-HRP-antirabbit (1:1000; 1 h, room temperature, EnVision kit, Dako). Detection was carried out with Lumi-Light^{PLUS}POD substrate (Roche).

Immunofluorescence staining

For double immunofluorescence staining the following antibodies were used: mouse monoclonal anti-DRP1 (1:200; Abcam), rabbit polyclonal anticatalase (1:200; Thermo Fisher Scientific, Rockford, Illinois, USA), mouse monoclonal antiporin (1:400; Abcam) and rabbit polyclonal antiporin (1:400; Abcam). All primary antibodies were diluted in Dako antibody diluent with background-reducing components (Dako, Glostrup, Denmark). The following secondary antibodies were used: antimouse Alexa Fluor 488 (1:500; Invitrogen, Eugene, Oregon, USA) and antirabbit Alexa Fluor 594 (1:1000; Invitrogen). Secondary antibodies were diluted in phosphate-buffered saline (PBS) containing 0.5% Tween 20 (PBS-T, pH 7.4).

Patient and control fibroblasts were allowed to attach overnight. After two washes with PBS, the cells were fixed overnight in neutral-buffered 4% formalin followed by heat-induced epitope retrieval in EDTA-T buffer (1 mM EDTA, pH 8.0, 0.05% Tween 20) for 40 min at 95°C and 20 min at room temperature. Sections were washed in deionised H_2O and equilibrated with PBS-T. Sections were incubated with primary antibodies for 1 h at room temperature. Afterwards, sections were washed three times in PBS-T and incubated for 1 h with secondary antibodies. Specimens were again washed three times in PBS-T and incubated with 0.5 µg/mL (4',6-diamidino-2-phenylindole (Sigma, St Louis, Missouri, USA) for 10 min. Slides were washed twice in distilled H_2O and mounted in Fluorescent Mounting Medium (Dako, Glostrup, Denmark).

Analysis of mitochondrial and peroxisomal morphology

Images were analysed using the image processing package Fiji.[18] Raw images were processed to remove the background and noise, and mitochondria were detected using the plugin tubeness. Images were then binarised, thresholded, skeletonised and subjected to particle analysis to acquire form factor (FF, 4π*area/perimeter^2) values and aspect ratio (AR) values derived from lengths of the major and minor axes. An AR value of 1 indicates a perfect circle, and AR increases as mitochondria elongate and become more elliptical. An FF value of 1 corresponds to a circular, unbranched mitochondrion, and higher FF values indicate a longer, more-branched mitochondrion. Quantitative analysis of peroxisome morphology was conducted on intermodes thresholded images after fast fourier transform (FFT) band filtering of the raw images and subjected to particle analysis. Peroxisomes were classified as either normal, elongated or juxtaposed elongated peroxisomes (JEPs).[19] Data were analysed using an unpaired two-tailed Student's t test.

RESULTS

Case reports

Patient 1

The boy was the first child of non-consanguineous Austrian parents; the family history was unremarkable. He was born at full term and of normal weight, length and head circumference

after a normal pregnancy, and postnatal adaptation was uncomplicated. At age 7 months he was admitted to hospital due to infantile spasms, and a subsequent EEG showed hypsarrhythmia. At that time the head circumference was microcephalic (1.5 cm less than the third percentile), he was severely hypotonic and showed few spontaneous movements, he was not grasping, fixating was reduced and tendon reflexes were normal. Lactate in plasma (<2.1 mmol/L) and cerebrospinal fluid (CSF) (<1.8 mmol/L) was normal, as was a brain MRI. Seizures responded well to antiepileptic medication and EEG was almost normalised. Despite continuous support, further motor and cognitive development remained very poor. At age 18 months a gastrostoma was inserted due to difficulties in swallowing and an external ophthalmoplegia became evident. Brain MRI at age 21 months revealed bilateral signal hyperintensities of the basal ganglia (putamen, pallidum) in T2-weighted images. At age 5 years, MRI changes became more prominent, with additional T2 signal hyperintensities in the caudate nucleus, subthalamic nucleus (figure 1, 1B) and dentate nucleus (figure 1C), and cerebellar atrophy was noted (figure 1E). MRC enzymes in muscle were normal (table 1).

Seizures relapsed, but barely compromised the patient. At age 7 years the boy was severely hypotonic without head and trunk control. Vision was severely impaired, and he only responded with smiling and crying. He was able to move his arms in a target-oriented manner, but was unable to grasp. Tendon reflexes were increased and muscle tone was stiff, and he required feeding via a gastric tube. Over the years, plasma lactate was mostly normal and only occasionally elevated, to a maximum of 4.1 mmol/L. The optic disc was pale, indicating optic nerve atrophy, and visual-evoked potentials were slowed (table 1). Motor nerve conduction velocities also were slowed and compound muscle action potential was reduced consistent with a mixed form of peripheral neuropathy. In addition, brain MRI at age 7 years showed increased T2 signalling of the optic radiation (figure 1D). Metabolic laboratory parameters for peroxisomal dysfunction, including very long chain fatty acids (VLCFAs), plasmalogens, phytanic acids and bile acid metabolites, were all within normal range (table 1).

Patient 2

The boy was the first child of consanguineous Turkish parents (first cousins). After a normal pregnancy, he was born at term by emergency caesarean section due to abnormal cardiotocography. The baby experienced severe asphyxia, with Apgar scores 1/4/6 and umbilical artery pH 6.92, and was resuscitated and ventilated for 6 days. Birth weight and head circumference were within normal ranges. Due to newborn seizures, he was treated with phenobarbital for 2 months. At age 4 months he presented with infantile spasms, head growth was microcephalic, brain

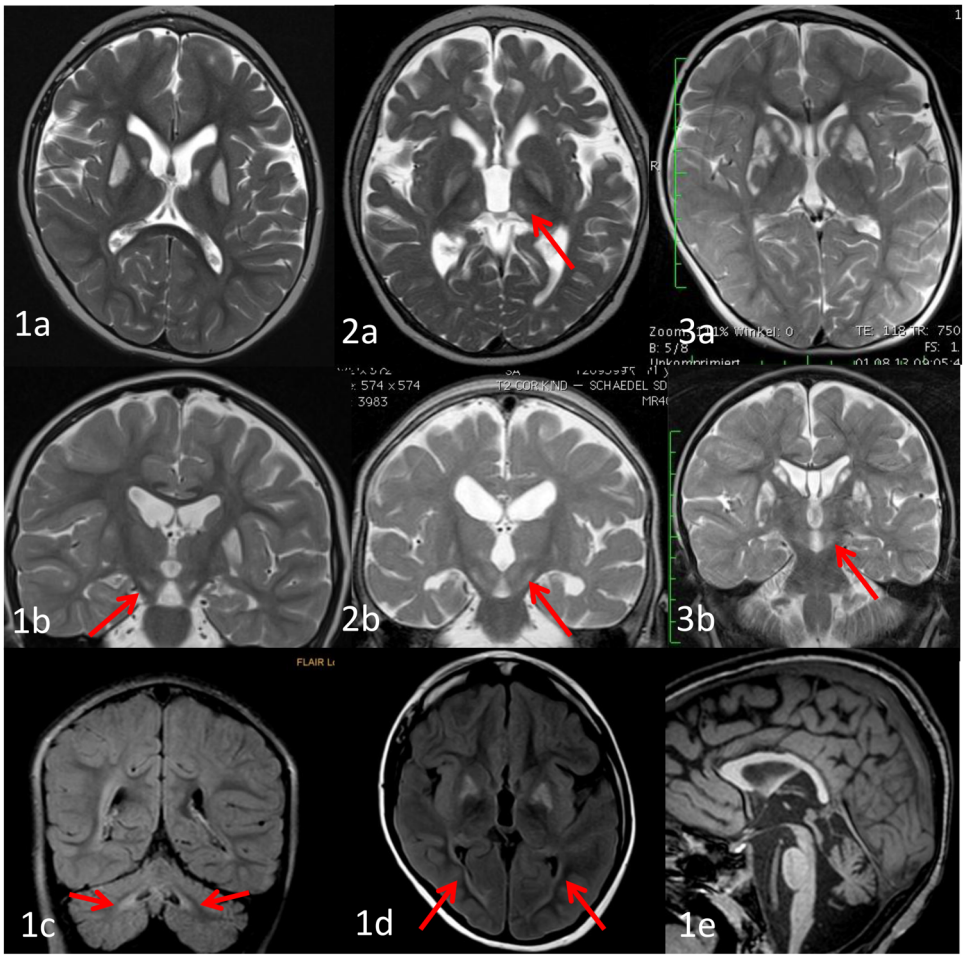

Figure 1 T2 and fluid attenuation inversion recovery (FLAIR) (1C –E) weighted images of patient 1 (1A, B: age 3 years; 1C,E: age 5 years; 1D: age 8 years), patient 2 (age 14 months) and patient 3 (age 2 years). Images illustrate increased signalling of basal ganglia (1A, 1B, 2A, 2B, 3A, 3B), thalamus (2A, arrow), subthalamic nucleus (1B, 2B, 3B, arrows), dentate nucleus (1C, arrows) and optic radiation (1D, arrows). Image 1E shows atrophy of the cerebellar vermis.

Table 1 Geneticfindings and phenotypic features of MFF-deficient patients

	Patient 1	Patient 2	Patient 3	Patient 4
Report	This paper	This paper	This paper	Shamseldin *et al*[10]
Family	1	2	2	3
Consanguinity	−	+	+	+
Origin	Austrian	Turkish	Turkish	Saudi Arabian
MFF variants	c.(184dup);(892C>T), p.(Leu62Profs*13);(Arg298*)	c.(453_454del);(453_454del), p.(Glu153Alafs*5);(Glu153Alafs*5)	c.(453_454del);(453_454del),p.(Glu153Alafs*5);(Glu153Alafs*5)	c.(190C>T);(190C>T) p.(Gln64*);(Gln64*))
Type of variant	Loss of function	Loss of function	Loss of function	Loss of function
Phenotypic features				
Sex	Male	Male	Male	Male
Age at onset	4 months	4 months	11 months	First year
Acquired microcephaly	+	+	+	Borderline microcephaly
Delayed motor milestones	+	+	+	+
Unable to sit independently	+	+	+	n.c.
GMFCS VI	+	+	+	n.c.
Muscular weakness	+	+	+	n.c.
Muscular hypotonia	+	+	+	n.c.
Increased tendon reflexes	+	+	+	+
Spasticity	+	+	+	+
Difficulties swallowing	+	+	+	n.c.
Gastric tube	+	+	−	n.c.
Growth retardation	−	−	+	n.c.
Verbal communication	−	−	−	+
Non-verbal communication	+	+	+	n.c.
Regression/loss of skills	+	+	+	n.c.
Abnormal EEG	+	+	+	n.c.
Hypsarrhythmia	+	+	+	n.c.
epileptic seizures	+	+	+	−
West syndrome	+	+	−	−
External ophthalmoparesis	+	+	+	−
Pale optic disc	+	−(9 months)	+	+
Visual impairment	+	+	+	−
Visual-evoked potentials abnormal	+	+	+	n.c.
Nerve conduction velocity abnormal	+	n.d.	+	n.c.
Reacting to noises	+	+	+	n.c.
Brain MRI				
Increased T2 signal				
Putamen	+	−	+	n.c.
Pallidum	+	+	+	+
Caudate nucleus	+	−	+	n.c.
Thalamus	−	+	+	n.c.
Mesencephalon	+	+	+	n.c.
Dentate nucleus	+	−	−	n.c.
Optic radiation	+	−	−	n.c.
Cerebellar atrophy, acquired	+	−	+	n.c.
Increased lactate MRS	−	n.d.	n.d.	n.c.
Laboratory findings				
Max. plasma lactate (mmol/L)	4.1	2.5	2.9	Normal
Increased lactate CSF	−	n.d.	n.d.	n.c.
MRC in muscle	Normal	n.d.	Normal	n.d.
MRC fibroblasts	n.d.	n.d.	n.d.	Normal
VLCFA increased	−	−	n.d.	−
Plasmalogens abnormal	−	n.d.	n.d.	n.d.
Pristanic acid abnormal	−	n.d.	n.d.	n.d.
Phytanic acid abnormal	−	n.d.	n.d.	n.d.
Bile acid metabolites abnormal	−	n.d.	n.d.	n.d.
Bone abnormalities	−	n.d.	n.d.	n.d.
Kidney cysts	−	n.d.	n.d.	n.d.

+, present; −, absent; CSF, cerebrospinal fluid; GMFCS, Gross Motor Function Classification System; MFF, mitochondrial fission factor; MRC, mitochondrial respiratory chain enzymes; MRS, magnetic resonance spectroscopy; n.c., not commented; n.d., not determined; VLCFA, very long chain fatty acids.

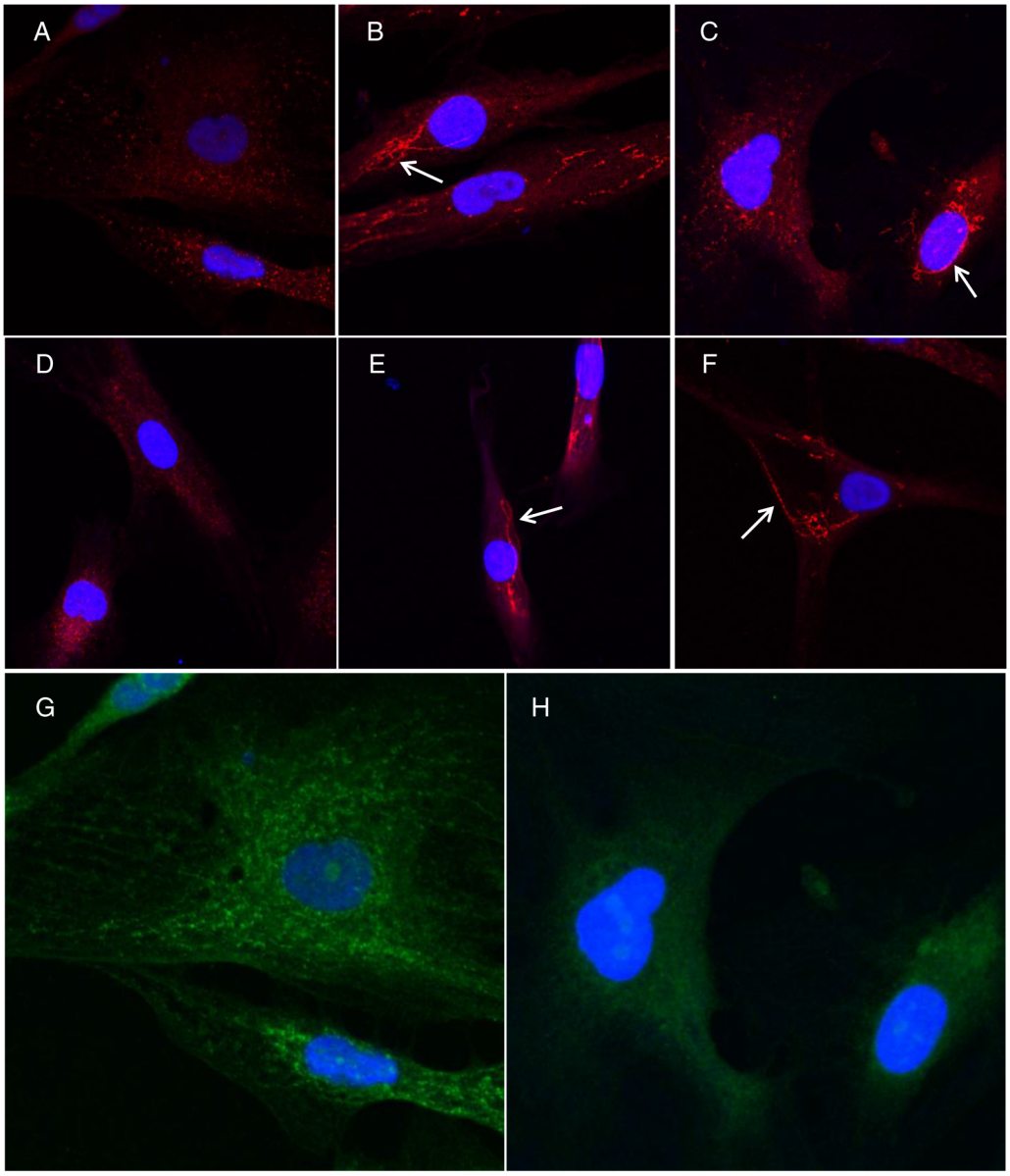

Figure 2 Immunofluorescence staining of catalase and dynamin-related protein 1 (DRP1) in mitochondrial fission factor (MFF) patient and control fibroblasts. (A–F) catalase; (G and H) DRP1; (A, D, G) control; (B, E) patient 1; (C, F, H) patient 3; white arrows point to giant peroxisomes in patient samples (B, C, E, F); small peroxisomes are visible in controls (A, D); localisation of DRP1 at distinct points in control cells (G); diffuse localisation of DRP1 in patient cells (H); magnification 63×.

MRI showed mild global atrophy but no specific posthypoxic changes, alanine in plasma was mildly elevated and serum lactate was normal. Despite extensive antiepileptic medication, the boy never became seizure-free. At age 9 months he was fixating, following with his eyes and reacting to his mother's voice and facial expressions with smiling and vocalising. He was severely hypotonic and never acquired trunk control. Brain MRI at age 14 months revealed bilateral increased T2 signalling of the globus pallidus, thalamus and subthalamic nucleus (figures 1 and 2A, B). At age 16 months, feeding via a gastric tube was started due to dysphagia, he had lost fixation and visual-evoked potentials were severely slowed (table 1), indicating optic atrophy. Nerve conduction velocity was not tested in this patient. The boy died at age 3 years due to respiratory failure.

Patient 3

The boy was the younger brother of patient 2. After a normal pregnancy he was born with normal birth weight, length, and head circumference, and his postnatal adaption was normal. At age 11 months the boy presented with developmental delay and microcephaly. He exhibited severe truncal hypotonia with increased tone in the limbs and normal tendon reflexes. He was able to fixate, follow with his eyes and respond to voices. EEG showed discontinuous hypsarrhythmia and subtle myoclonic seizures. Under antiepileptic medication the seizures stopped and EEG normalised. In his second year of life he displayed external ophthamoplegia. Brain MRI showed bilateral increased T2 signalling of basal ganglia (putamen, caudate nucleus) and the subthalamic nucleus (figures 1 and 3A, B) and the first signs of cerebellar atrophy. At age 4 years he was severely hypotonic without trunk control, was able to fixate and follow with his eyes and his tendon reflexes were increased. He had dysphagia, but a gastric tube was denied by the parents. Lactate was normal or minimally elevated (up to 2.5 mmol/L), and VLCFA was not tested. Visual-evoked potentials were negative and optic discs were pale, indicating optic atrophy (table 1). Motor nerve

conduction velocity was slowed with compound muscle action potential within normal ranges, consistent with demyelinating peripheral neuropathy.

Exome sequencing reveals truncating biallelic *MFF* variants

In a first filtering step we focused on rare (MAF<0.1% in 6000 control exomes) homozygous or potentially compound heterozygous non-synonymous variants. This search identified 15 and 36 different genes in patients 1 and 3, respectively. Two and five of these genes were listed in OMIM with a phenotype key of 3, and have been associated with autosomal recessive or X-linked inherited disorders. None of the variants in these OMIM genes were considered as likely to be clinically relevant. In a second step we prioritised rare predictively biallelic loss-of-function variants in genes coding for mitochondrial proteins. In both patients, *MFF* was the only remaining candidate with no such variants being identified in 6000 control exomes. Sanger sequencing confirmed the variants, which in the two families segregated in a pattern compatible with a recessively inherited condition. The *MFF* variant c.892C>T, p.(Arg298*) has been listed once in a heterozygous state in 121 244 control alleles of the Exome Aggregation Consortium (ExAC) Server (08/2015). All other variants were absent from 6000 control exomes of an in-house database and public databases (dbSNP, Washington Exom Variant Server (EVS), ExAC Server (08/2015)). These findings support the clinical relevance of the identified *MFF* variants.

Biochemical studies of muscle

No significant alterations of the oxidative phosphorylation complex activities were found in the patients compared with controls (table 1). Long-range PCR analysis of mitochondrial DNA of patient 3 revealed no deletions.

Immunoblotting

DRP1 amounts were normal in patients compared with controls, as indicated by western blot analysis (figure 3A). In addition, no significant alterations of porin (figure 3A) (marker for the mitochondria) and catalase (figure 3A) (marker for peroxisomes) were detected.

Immunofluorescence staining

Immunofluorescence staining of fibroblasts revealed a distinct staining pattern of DRP1 in patients 1 and 3 versus controls. The patients showed a diffuse staining (figure 2H), whereas in control fibroblasts DRP1 was concentrated in specific spots (figure 2G).

Quantitative analysis of peroxisomes

Extremely elongated peroxisomes were found in fibroblasts of patients 1 and 3 (figure 2B, C, E, F) compared with controls (figure 2A, D), as indicated by catalase immunostaining. In controls, many punctate reactivities were present, whereas in the patients' fibroblasts, few giant peroxisomes were visible. The bar graph (figure 3B) shows the reduction in the proportion of normal peroxisomes and increases in the proportions of elongated and very elongated (JEPs, p value <0.0001) peroxisomes in patient cells versus control cells.

Quantitative analysis of mitochondria

A significant increase of mitochondrial branching (FF, form factor; p value 1.2e−7) and AR (p value 1.9e−25) in the patient group versus the control group was found. Plotting AR against FF revealed that particles analysed from MFF-derived cells have higher values of both FF and AR (figure 4). These high values indicate that patients' mitochondria were significantly elongated, as indicated by porin staining, compared with mitochondria of normal fibroblasts (figure 4I, L). The mitochondrial strands of the patients were long and interconnected, giving a continuous network. In contrast, the mitochondria of control cells were short and frequently interrupted.

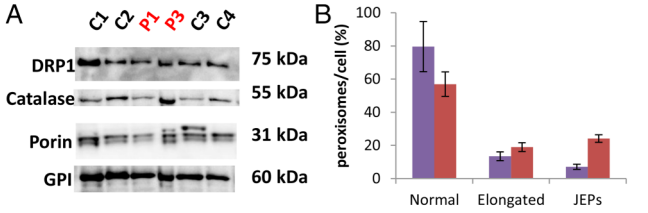

Figure 3 (A) Immunoblot analysis of the content of mitochondria, peroxisomes and dynamin-related protein 1 (DRP1) in mitochondrial fission factor (MFF)-mutated patients. C1–C4: control muscle; P1, P3: patient muscle; glucose-6-phosphate isomerase (GPI) was used as a loading control. (B) Bar graph showing the decrease in percentage of normal peroxisomes and the increase of the elongate and very elongated (juxtaposed elongated peroxisomes (JEPs), p value<0.0001) in the patient group versus the control group. Purple, controls; red, patients.

DISCUSSION

The clinical phenotype of the three boys was characterised by disease onset in the first year of life, which manifested as seizures, developmental delay and acquired microcephaly; in subsequent years, dysphagia, spasticity, optic neuropathy and peripheral neuropathy developed (table 1). The clinical phenotype of our three patients partially overlaps with that of the first boy characterised with an *MFF* mutation in 2012,[11] except for the seizures and dysphagia. That first-described patient had an apparently milder course, but because his clinical features were not described in detail, a fuller comparison is not possible. In our patients, bilateral basal ganglia and brainstem changes on brain MRI (figure 1) in the second year of life led to the differential diagnosis of mitochondrial disease, even though lactate was normal in plasma, CSF and on MRI spectroscopy. The course of the disease was slowly progressive, without crisis. MRC enzymes in muscle biopsy were normal. Exome sequencing revealed the molecular defect in each case, with patient 2 diagnosed retrospectively.

All three patients were found to have truncating mutations in *MFF*, resulting in mitochondrial and peroxisomal biogenesis defects, as proven by the results of porin (figure 4G, H) and catalase (figure 2B, C, E, F) immunostaining. Extremely elongated and interconnected mitochondria and peroxisomes were observed in fibroblasts of patients 1 and 3 (figures 2B, C, E, F, 3B and 4G, H). Immunoblot analysis revealed normal contents of mitochondria and peroxisomes (figure 3A). DRP1, a binding partner of MFF, was present in normal amounts, as indicated by western blot analysis (figure 3A). However, we found different cellular localisations of DRP1 between the patients and controls. In controls, DRP1 was localised at very distinct points (figure 2G), which likely represent the nodes were mitochondrial and peroxisomal fission is initiated. In the two patients examined, DRP1 showed a diffuse staining pattern (figure 2H), suggesting that DRP1 is not recruited to the fission nodes, as MFF is thought to be the major DRP1 receptor during organelle fission.[2] We assume that enlarged mitochondria and peroxisomes are ill-suited for axonal transport, especially in

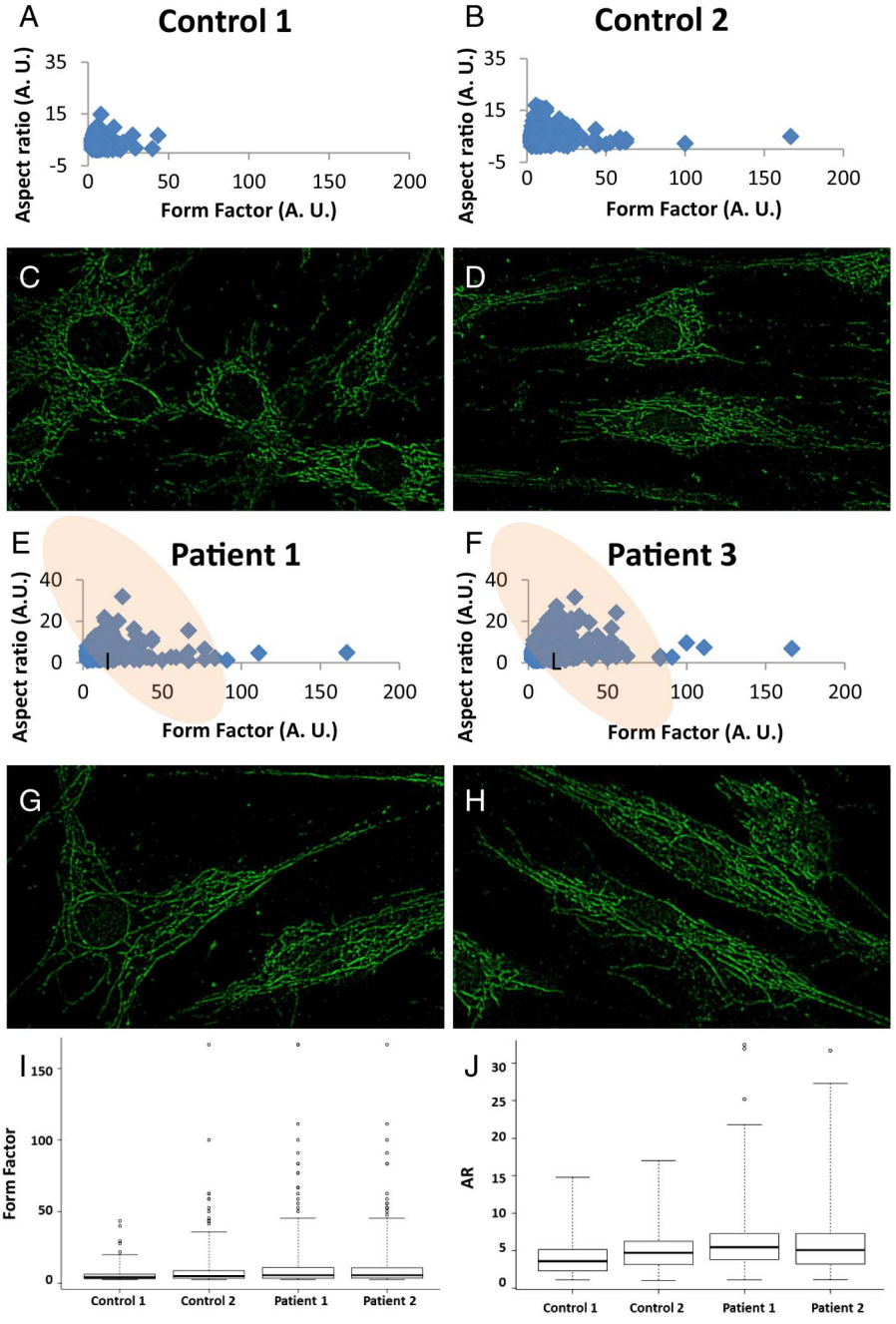

Figure 4 Mitochondrial morphology in control and mitochondrial fission factor (MFF)-mutant fibroblasts. Plotting aspect ratio (AR) against form factor (FF) shows that the particles analysed from the MFF-derived cells have higher values of FF and AR. These high values indicate that mitochondria are bigger and more elongated in these cells. (A) control 1; (B) control 2; (E) patient 1; (F) patient 3. (C, D, G, H) Porin staining with background correction; (C) control 1; (D) control 2; (G) patient 1; (H) patient 3; 63×magnification, (I–J) box-and-whisker plot showing the significant increase of mitochondrial branching (FF, form factor), p value 1.2×10^{-7} and (C) AR, p value: 1.9×10^{-25} in the patient sample versus the control sample.

neurons. In addition, delivery to other, even smaller protuberances in the brain might be disturbed. For example, fine astrocyte processes were reported to contain very small mitochondria.[20] The authors of that study speculated that glial oxidative capability may fuel transmitter metabolism. Primary culture of neural cell-specific Drp1−/− mouse forebrain showed a reduced number of neurites and defective synapse formation, thought to be due to aggregated mitochondria that failed to distribute properly within the cell processes.[21] Interestingly, it was reported that a Bcl-xL-Drp1 complex regulates synaptic vesicle membrane dynamics during endocytosis and depends on mitochondrial ATP.[22] Therefore, improper recruitment of DRP1 might enhance neuronal perturbation. Importantly, MFF was reported to mediate DRP1 recruitment to synaptic vesicles.[23] Clinically early signs of impaired neuronal function, including reduced nerve conduction velocity, delayed visual-evoked potentials and optic nerve atrophy, were documented in all three boys (table 1). An interesting finding on brain MRI was the increased signalling of the optic radiation in fluid attenuation inversion recovery-weighted images of patient 1 (figure 1D). White matter hyperintensities along the optic radiation have been found to be focal or distributed in patients with optic nerve atrophy due to *OPA1* mutations, a gene involved in mitochondrial fusion.[24] Cerebellar atrophy was observed as a subsequent sign and was most distinct in patient 1 (figure 1E) and at an early stage in patient 3. Cerebellar atrophy and increased T2 signalling (dentate nucleus in patient 1, figure 1C) are common findings in patients with mitochondrial disease[25] and have been described as well in patients with mutations in genes involved in mitochondrial dynamics such as *SLC25A46* (optic atrophy and CM T type

2 disease)[26] and in patients with *OPA1* mutations.[27] In contrast to *OPA1* patients, no deletions of mtDNA were identified in muscle sample from patient 3.

Similarly, enlarged peroxisomes might also be disruptive to the nervous system. Peroxisomes in the brain have been reported to be very small, so-called microperoxisomes.[28] Most peroxisomes of neurons are located in the soma; however, peroxisomes are also frequently found in the cellular processes of astrocytes, oligodendrocytes and microglia. They are rarely found in axons and synaptic terminals.[28–30] Developmental delay, impaired vision, generalised muscular hypotonia, failure to thrive and epileptic seizures are the main features of the three patients presented here, compatible with peroxisomal biogenesis disorders (PBD). However, more specific signs of early-onset PBD such as facial abnormalities (macrocephaly, high forehead, frontal bossing), typical brain MRI findings (malformations of cortical development, leukodystrophy) and signs of impaired liver function were not found in our patients. Furthermore, biochemical parameters for PBD (VLCFA, plasmalogens, phytanic acid, pristanic acid, bile acid metabolites) were within normal ranges (table 1).

In summary, we described for the first time detailed clinical and functional data of three patients with a mitochondrial and peroxisomal biogenesis defect due to loss-of-function mutations in *MFF*. The clinical phenotypes of the three boys are quite similar (table 1) and structural pathology of the organelles is evident (figures 2 and 3). Noteworthy biochemical parameters for mitochondrial and peroxisomal function are within normal ranges (table 1). We conclude that in early-onset Leigh-like basal ganglia disease with seizures along with early-onset optic and peripheral neuropathy, diagnostic workup should include investigation of *MFF*. Further studies are needed to clarify the specific mode of damage as a consequence of the organellar structural abnormalities.

Author affiliations
[1]Department of Pediatrics, Paracelsus Medical University Salzburg, Salzburg, Austria
[2]Department of Pediatrics, Kreisklinken Reutlingen, Reutlingen, Germany
[3]Social Paediatric Center, Klinikum Frankfurt-Höchst, Frankfurt am Main, Germany
[4]Department of Ophthalmology and Optometry, Department of Anatomy, Department of Laboratory Medicine (HW), and First Department of Internal Medicine, Paracelsus Medical University, Salzburg, Austria
[5]Institute of Human Genetics, Helmholtz Zentrum München, Neuherberg, Germany
[6]Institute of Human Genetics, Klinikum rechts der Isar, Technische Universität München, Munich, Germany

Acknowledgements We thank Professor Eugen Boltshauser (Zurich) for evaluation of the MRI images.

Contributors JK: patient recruitment, data collection, analysis of clinical and imaging data, study conception and design, manuscript drafting. RGF: biochemical and molecular genetic studies, manuscript drafting. PF: patient recruitment, data collection, analysis of clinical and imaging data, manuscript drafting. MP: patient recruitment, data collection, analysis of clinical and imaging data, manuscript drafting. FS: fluorescence microscopy. AI: investigation of mitochondrial morphology. WS: study conception and design, manuscript drafting. JAM: study conception and design, manuscript drafting, biochemical and molecular genetic studies. HP: biochemical and molecular genetic studies, manuscript drafting. TBH: biochemical and molecular genetic studies, study conception and design, manuscript drafting. All authors revised the manuscript critically and approved the final version.

Funding Salzburg Center Foundation, the 'Vereinigung zur Förderung der pädiatrischen Forschung und Fortbildung'. This study was supported by the German Bundesministerium für Bildung und Forschung (Bundesministerium für Bildung und Forschung, Germany) through the German Network for mitochondrial disorders (mitoNET; 01GM1113C to HP) and through the E-Rare project GENOMIT (01GM1207 for HP). TBH was supported by the Bundesministerium für Bildung und Forschung, Germany through the Juniorverbund in der Systemmedizin 'mitOmics' (FKZ 01ZX1405C) and WS by the Add-On-Project A-12/01/005-SPE of the PMU-FFF.

Competing interests None declared.

Ethics approval All procedures were in accordance with the ethical standards of the responsible committee on human experimentation (institutional and national) and with the Helsinki Declaration of 1975, as revised in 2013. All clinical data and samples were obtained with written informed consent of the patients' parents. The ethics committee of Technische Universität München approved the exome sequencing studies.

Provenance and peer review Not commissioned; externally peer reviewed.

REFERENCES

1 Richter V, Palmer CS, Osellame LD, Singh AP, Elgass K, Stroud DA, Sesaki H, Kvansakul M, Ryan MT. Structural and functional analysis of MiD51, a dynamin receptor required for mitochondrial fission. *J Cell Biol* 2014;204:477–86.
2 Schrader M, Costello J, Godinho LF, Islinger M. Peroxisome-mitochondria interplay and disease. *J Inherit Metab Dis* 2015;38:681–702.
3 Waterham HR, Koster J, van Roermund CW, Mooyer PA, Wanders RJ, Leonard JV. A lethal defect of mitochondrial and peroxisomal fission. *N Engl J Med* 2007;356:1736–41.
4 Westermann B. Organelle dynamics: ER embraces mitochondria for fission. *Curr Biol* 2011;21:R922–4.
5 Song M, Mihara K, Chen Y, Scorrano L, Dorn GW 2nd. Mitochondrial fission and fusion factors reciprocally orchestrate mitophagic culling in mouse hearts and cultured fibroblasts. *Cell Metab* 2015;21:273–85.
6 Bonekamp NA, Sampaio P, de Abreu FV, Luers GH, Schrader M. Transient complex interactions of mammalian peroxisomes without exchange of matrix or membrane marker proteins. *Traffic* 2012;13:960–78.
7 Long B, Wang K, Li N, Murtaza I, Xiao JY, Fan YY, Liu CY, Li WH, Cheng Z, Li P. miR-761 regulates the mitochondrial network by targeting mitochondrial fission factor. *Free Radic Biol Med* 2013;65:371–9.
8 Pareyson D, Saveri P, Sagnelli A, Piscosquito G. Mitochondrial dynamics and inherited peripheral nerve diseases. *Neurosci Lett* 2015;596:66–77.
9 Gandre-Babbe S, van der Bliek AM. The novel tail-anchored membrane protein Mff controls mitochondrial and peroxisomal fission in mammalian cells. *Mol Biol Cell* 2008;19:2402–12.
10 Losón OC, Song Z, Chen H, Chan DC. Fis1, Mff, MiD49, and MiD51 mediate Drp1 recruitment in mitochondrial fission. *Mol Biol Cell* 2013;24:659–67.
11 Shamseldin HE, Alshammari M, Al-Sheddi T, Salih MA, Alkhalidi H, Kentab A, Repetto GM, Hashem M, Alkuraya FS. Genomic analysis of mitochondrial diseases in a consanguineous population reveals novel candidate disease genes. *J Med Genet* 2012;49:234–41.
12 Haack TB, Hogarth P, Kruer MC, Gregory A, Wieland T, Schwarzmayr T, Graf E, Sanford L, Meyer E, Kara E, Cuno SM, Harik SI, Dandu VH, Nardocci N, Zorzi G, Dunaway T, Tarnopolsky M, Skinner S, Frucht S, Hanspal E, Schrander-Stumpel C, Heron D, Mignot C, Garavaglia B, Bhatia K, Hardy J, Strom TM, Boddaert N, Houlden HH, Kurian MA, Meitinger T, Prokisch H, Hayflick SJ. Exome sequencing reveals de novo WDR45 mutations causing a phenotypically distinct, X-linked dominant form of NBIA. *Am J Hum Genet* 2012;91:1144–9.
13 Berger A, Mayr JA, Meierhofer D, Fotschl U, Bittner R, Budka H, Grethen C, Huemer M, Kofler B, Sperl W. Severe depletion of mitochondrial DNA in spinal muscular atrophy. *Acta Neuropathol* 2003;105:245–51.
14 Feichtinger RG, Weis S, Mayr JA, Zimmermann F, Geilberger R, Sperl W, Kofler B. Alterations of oxidative phosphorylation complexes in astrocytomas. *Glia* 2014;62:514–25.
15 Meierhofer D, Mayr JA, Foetschl U, Berger A, Fink K, Schmeller N, Hacker GW, Hauser-Kronberger C, Kofler B, Sperl W. Decrease of mitochondrial DNA content and energy metabolism in renal cell carcinoma. *Carcinogenesis* 2004;25:1005–10.
16 Rustin P, Chretien D, Bourgeron T, Gérard B, Rötig A, Saudubray JM, Munnich A. Biochemical and molecular investigations in respiratory chain deficiencies. *Clin Chim Acta* 1994;228:35–51.
17 Mayr JA, Merkel O, Kohlwein SD, Gebhardt BR, Bohles H, Fotschl U, Koch J, Jaksch M, Lochmuller H, Horvath R, Freisinger P, Sperl W. Mitochondrial phosphate-carrier deficiency: a novel disorder of oxidative phosphorylation. *Am J Hum Genet* 2007;80:478–84.
18 Schindelin J, Arganda-Carreras I, Frise E, Kaynig V, Longair M, Pietzsch T, Preibisch S, Rueden C, Saalfeld S, Schmid B, Tinevez JY, White DJ, Hartenstein V, Eliceiri K, Tomancak P, Cardona A. Fiji: an open-source platform for biological-image analysis. *Nat Methods* 2012;9:676–82.
19 Koch J, Brocard C. PEX11 proteins attract Mff and human Fis1 to coordinate peroxisomal fission. *J Cell Sci* 2012;125(Pt 16):3813–26.
20 Derouiche A, Haseleu J, Korf HW. Fine astrocyte processes contain very small mitochondria: glial oxidative capability may fuel transmitter metabolism. *Neurochem Res* 2015;40:2402–13.
21 Ishihara N, Nomura M, Jofuku A, Kato H, Suzuki SO, Masuda K, Otera H, Nakanishi Y, Nonaka I, Goto Y, Taguchi N, Morinaga H, Maeda M, Takayanagi R, Yokota S, Mihara K. Mitochondrial fission factor Drp1 is essential for embryonic development and synapse formation in mice. *Nat Cell Biol* 2009;11:958–66.
22 Li H, Alavian KN, Lazrove E, Mehta N, Jones A, Zhang P, Licznerski P, Graham M, Uo T, Guo J, Rahner C, Duman RS, Morrison RS, Jonas EA. A Bcl-xL-Drp1 complex regulates synaptic vesicle membrane dynamics during endocytosis. *Nat Cell Biol* 2013;15:773–85.

23 Otera H, Wang C, Cleland MM, Setoguchi K, Yokota S, Youle RJ, Mihara K. Mff is an essential factor for mitochondrial recruitment of Drp1 during mitochondrial fission in mammalian cells. *J Cell Biol* 2010;191:1141–58.

24 Rocca MA, Bianchi-Marzoli S, Messina R, Cascavilla ML, Zeviani M, Lamperti C, Milesi J, Carta A, Cammarata G, Leocani L, Lamantea E, Bandello F, Comi G, Falini A, Filippi M. Distributed abnormalities of brain white matter architecture in patients with dominant optic atrophy and OPA1 mutations. *J Neurol* 2015;262:1216–27.

25 Delonlay P, Rötig A, Sarnat HB. Respiratory chain deficiencies. *Handb Clin Neurol* 2013;113:1651–66.

26 Abrams AJ, Hufnagel RB, Rebelo A, Zanna C, Patel N, Gonzalez MA, Campeanu IJ, Griffin LB, Groenewald S, Strickland AV, Tao F, Speziani F, Abreu L, Schule R, Caporali L, La Morgia C, Maresca A, Liguori R, Lodi R, Ahmed ZM, Sund KL, Wang X, Krueger LA, Peng Y, Prada CE, Prows CA, Schorry EK, Antonellis A, Zimmerman HH, Abdul-Rahman OA, Yang Y, Downes SM, Prince J, Fontanesi F, Barrientos A, Nemeth AH, Carelli V, Huang T, Zuchner S, Dallman JE. Mutations in SLC25A46, encoding a UGO1-like protein, cause an optic atrophy spectrum disorder. *Nat Genet* 2015;47:926–32.

27 Roubertie A, Leboucq N, Picot MC, Nogue E, Brunel H, Le Bars E, Manes G, Angebault Prouteau C, Blanchet C, Mondain M, Chevassus H, Amati-Bonneau P, Sarzi E, Pages M, Villain M, Meunier I, Lenaers G, Hamel CP. Neuroradiological findings expand the phenotype of OPA1-related mitochondrial dysfunction. *J Neurol Sci* 2015;349:154–60.

28 Kassmann CM. Myelin peroxisomes—essential organelles for the maintenance of white matter in the nervous system. *Biochimie* 2014;98:111–8.

29 Holtzman E, Teichberg S, Abrahams SJ, Citkowitz E, Crain SM, Kawai N, Peterson ER. Notes on synaptic vesicles and related structures, endoplasmic reticulum, lysosomes and peroxisomes in nervous tissue and the adrenal medulla. *J Histochem Cytochem* 1973;21:349–85.

30 Kassmann CM, Quintes S, Rietdorf J, Mobius W, Sereda MW, Nientiedt T, Saher G, Baes M, Nave KA. A role for myelin-associated peroxisomes in maintaining paranodal loops and axonal integrity. *FEBS Lett* 2011;585:2205–11.

Disturbed mitochondrial and peroxisomal dynamics due to loss of MFF causes Leigh-like encephalopathy, optic atrophy and peripheral neuropathy

Johannes Koch, René G Feichtinger, Peter Freisinger, Mechthild Pies, Falk Schrödl, Arcangela Iuso, Wolfgang Sperl, Johannes A Mayr, Holger Prokisch and Tobias B Haack

J Med Genet 2016 53: 270-278 originally published online January 18, 2016
doi: 10.1136/jmedgenet-2015-103500